Supplementary Information for:

High-performance Hg^{2+} FET-type sensors based on reduced graphene oxide/polyfuran nanohybrids

Jin Wook Park,[a] *Seon Joo Park*,[a] *Oh Seok Kwon*,[b] *Choonghyeon Lee*,[a] and *Jyongsik Jang**[a]

[a] World Class University (WCU) program of Chemical Convergence for Energy & Environment (C2E2), School of Chemical and Biological Engineering, College of Engineering, Seoul National University (SNU), Seoul, Korea.

[b] Dr. O. S. Kwon

Department of Chemical and Environmental Engineering School of Engineering and Applied Science Yale University, New Haven, USA.

*Corresponding Authors: E-mail: jsjang@plaza.snu.ac.kr, Fax: (+82) 2-888-1604, Tel: (+82) 2-880-7069

Experimental Section

Materials: Furan (99 %), Mercury (II) nitrite monohydrate (98%), sodium nitrite, cobalt (II) n itrite hexahydrate, nickel(II) nitrite hex ahydrate, zinc nitrite hexahydrate, lithium nitrate, pall adium (IV) chloride, copper (II) nitrate trihydrate, cerium (IV) sulfate, graphite flakes, methyl orange (MO), and ferric chloride ($FeCl_3$, 97 %) were purchased from Aldrich Chemical Co. a nd used without further purification.

*Synthesis of 1-D PF nanomaterials***:** A self-degraded template method was carried out for the preparation of PF NTs.[1] Firstly, $FeCl_3$ (0.243 g, 1.5 mmol) was added to a 5-mM MO solutio n (sodium 4-[4′-(dimethylamino)phenyldiazo] phenylsulfonate, $(CH_3)2NC_6H_4$-N=$NC_6H_4SO_3$ Na) in deionized water. After a flocculent precipitate appeared, the furan monomer (102 mg, 1.5 mmol) was added. The mixture was then stirred at room temperature for 24 hours. The res ulting precipitate was purified by washing it with deionized water and methanol several times until the filtrate was colorless and had a neutral pH. Finally, the powdered PF NTs (80 mg, 78.4 %) were dried under vacuum at 60°C for 24 hours.

Synthesis of rGO-PF nanocomposites: GO was obtained from graphite powder using a modifi ed Hummers and Offeman method.[2] GO (4 mg/mL) was dispersed in deionized water and the n mixed with PF NTs (4 mg). The mixtures were ultrasonicated for 1 hour. The 5 μL (35 wt %) hydrazxine solution exposed to the resulting GO-PF NT structures for 1 hour at 95°C, leadin g to reduction process from GO to rGO. The final product, the rGO-PF NT composite (6.5 m g, 81.3 %), was obtained via purification by using water, filtration, and dried in a vacuum ove n at 25°C for hours.

Fabrication of rGO-PF NT composite FET sensor: A microarray (80 pairs of gold interdigitated microelectrodes) was patterned on a glass substrate using a 50-nm-thick Cr adhesion layer via a photolithographic process, resulting in electrodes with a gold layer thickness of 50 nm, a width of 10 μm, length of 4000 μm, and an interelectrode spacing of 10 μm. The microelectrode substrate was washed using sonication in ethanol. An aliquot of 0.1 mL of the ethanol solution containing 0.1 wt % rGO-PF NT composites was dropped onto the patterned electrodes. Then, the microelectrode substrate was dried under vacuum at room temperature for several hours. A solution chamber (volume 10 mL) was designed and employed for all liquid-based measurements. The FET sensor substrate based on liquid-ion gate was fabricated with phosphate-buffered solution (PBS, pH 7.5).

Instrumentation: The TEM images were obtained with a JEOL JEM-2100 microscope. For TEM observation, the samples were diluted with ethanol and then the diluted solution was deposited on a copper grid coated with a carbon film. The FE-SEM images were taken with a JEOL JSM-6700 F microscope. A specimen was coated with a thin layer of gold to eliminate charging effects. Raman spectra were recorded with a T64000 (Horiba Jobin Yvon). ATR-FTIR spectra were collected with a Thermo Scientific Nicolet 6700 FTIR spectrophotometer. X-ray diffraction (XRD) patterns were carried out with a New D8 Advance (Bruker). All electrical measurements were conducted with a Keithley 2612A sourcemeter, a probe station (MS TECH, MODEL 4000) and a Wonatech WBCS 3000 potentiostat.

To gain insight into the structure of the graphene–PF NT composites, Raman spectroscopy was carried out, and the resulting spectra are shown in Fig. S1a. The Raman spectrum of GO contained D peaks at 1364 cm^{-1} and G peaks at 1610 cm^{-1}. The Raman spectrum of the rGO exhibited two prominent bands at 1343 cm^{-1} and 1592 cm^{-1}, which correspond to D and G bands. The ratio of the D band to G band (I_d/I_G) was minimally greater than that of GO, suggesting that the reduction process induced defects or edge areas in the rGO sheets. The Raman spectrum of PF NTs contained a C=C backbone stretching peak at ~ 1590 cm^{-1} and a PF ring stretching peak at 1410 cm^{-1}. The Raman spectrum of the rGO–PF NT hybrids exhibited increased intensity of the band around 1350 cm^{-1}, indicating an interaction between PF and the rGO sheets.

The structure of the rGO–PF NTs was further studied using X-ray diffraction (XRD) and attenuated total reflectance (ATR) Fourier transform infrared (FTIR) spectroscopy, as shown in Figs. S1b and S1c. The XRD diffractograms of GO contained a very sharp peak at 10.1° (d = 8.75 Å), which indicated that the structure of the original graphite was successfully oxidized to form GO. A broad peak appeared at 24.8° (d = 3.59 Å), which implied that rGO formation was achieved by hydrazine reduction of GO. The graphene–PF NT hybrids contained a broad peak at approximately 25.3° (d = 3.52 Å), which corresponded to the furan intermolecular distance between the rGO–PF NTs. This result suggested that the PF NTs and the rGO sheet formed a composite via π–π interactions.

GO exhibited characteristic oxide absorption bands, including the C=O stretching peak at 1733 cm^{-1}, the vibrational and deformation peaks of O-H groups at 3391 cm^{-1} and 1417 cm^{-1}, and the C-O (alkoyl) stretching peak at 1037 cm^{-1} (see Fig. S1b). Most of the peaks related to oxygen-containing functional groups vanished in the FTIR spectrum of rGO, thus indicating that the reduction of GO was successful. The spectrum of the rGO–PPy NT composite

material contained characteristic furan ring and graphene fundamental vibrations: 1598 cm^{-1} (C=C stretching); 1512 and 1498 cm^{-1} (C-C stretching); 1026 and 1001 cm^{-1} (C-O-C plane deformation); and 1149, 1096, and 1052 cm^{-1} (C-H bending and stretching). The peaks in the spectrum of the rGO–PF NT composites were shifted compared with those of the separate PF NTs and rGO spectra due to interactions between the rGO layers and PF NTs.

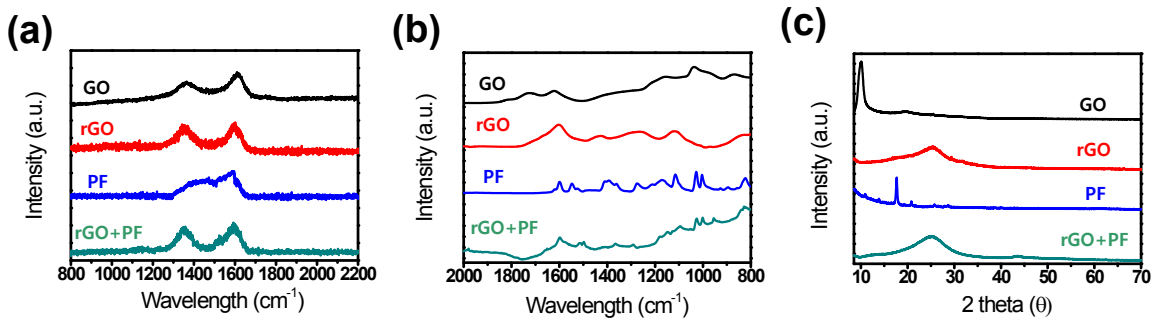

Fig. S1 (a) Raman, (b) ATR-FT-IR spectra, and (c) X-ray diffraction patterns of GO, rGO, P F, and rGO+PF NT composites.

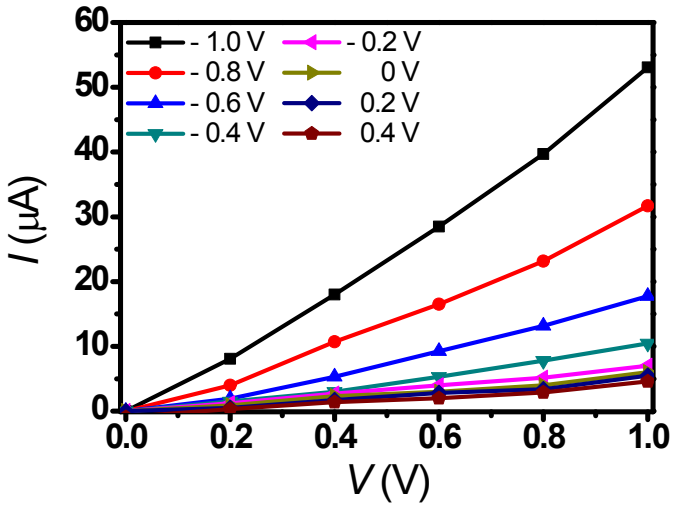

Fig. S2 PF NTs at V_g from −1.0 to 0.4 V in 0.2-V steps (Vsd: 0 to 1.0 V in 0.2-V steps).

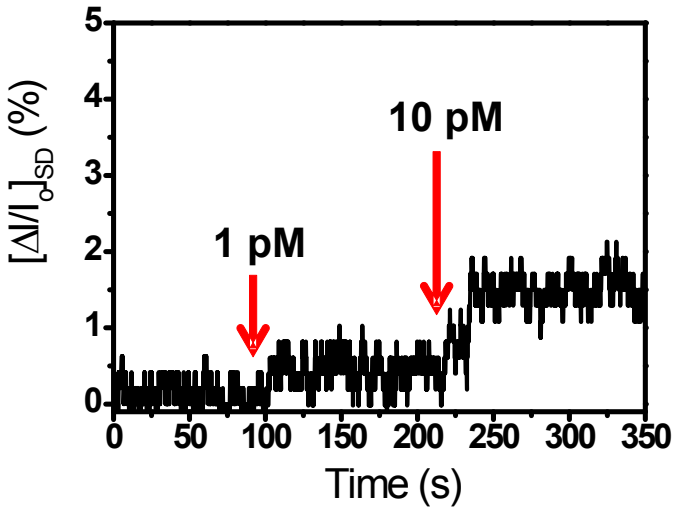

Fig. S3 Real-time responses for Hg^{2+} sensor based on rGO-PF NT composites measured at V_{sd} = 10 mV (V_g = - 0.1 V) with a Hg^{2+} concentration of 1 pM to 10 pM.

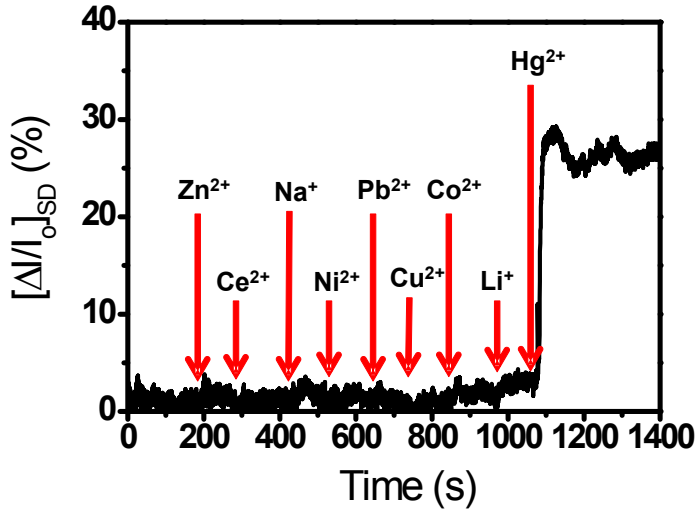

Fig. S4 Real-time responses to Zn^{2+}, Ce^{2+}, Na^{+}, Ni^{2+}, Pb^{2+}, Cu^{2+}, Co^{2+}, Li^{+}, and Hg^{2+} measured at V_{SD}= 10 mV (V_g = - 0.1 V).

Table S1. Comparison of the mercury sensing performance of various sensor type devices.

Electrode materials	Sensor type	Sensitivity (μM)	Reference
CNT	Vapor	1	3
Ni/Au NHs	Vapor	0.1	4
PPy/Pd NHs	Vapor	1	5
CNT/Au NPs	Vapor	0.002	6
rGO/PSe NCs	LE FET	0.000001	In this work

CNT = Carbon nanotube, NP = Nanoparticle, LE FET = Liquid electrolyte field effect transistor, NH = Nanohybrid

Reference

1. X. Yang, Z. Zhu, T. Dai and Y. Lu, *Macromol. Rapid Commun.* 2005, **26**, 1736.

2. W. S. Hummers and R. E. Offeman, *J. Am. Chem. Soci.* 1958, **80**, 1339.

3. A. Safavi, N. Maleki, M. M. Doroodmand, *J. Hard. Mater.* **2010***, 173,* 622.

4. Y. M. Sabri, S. J. Ippolito, A. J. Atanacio, V. Bansal, S. K. Bhargava, *J. Mater. Chem.,* **2012***, 22,* 21395.

5. Y. M. Sabri, R. Kojima, S. J. Ippolito, W. Wlodarski, K. Kalantar-zadeh, R. B. Kaner, S. K. Bhargava, *Sens. Actuators B,* **2011***, 160,* 616.

6. T. P. McNicholas, K. Zhao, C. Yang, S. C. Hernandez, A. Mulchandani, N. V. Myung and M. A. Deshusses, *J. Phys. Chem. C*, 2011, **115**, 13927.